

A survey of the synchronization process of synchronous generators and power electronic converters

W. JARZYNA*

Faculty of Electrical Engineering and Computer Science, Lublin University of Technology, 38A Nadbystrzycka St., 20-618 Lublin, Poland

Abstract. The process of synchronization of synchronous generators and power electronic converters with the power grid may take on quite different forms. This is due to their specific principles of operation and essential differences in energy conversion process. However, since synchronous generators and power converter often operate in the same utility network, coherent rules should be defined for them. Therefore, this paper aims at a formulation of the uniform and consistent interpretation of synchronization with the power grid for both types of aforementioned units. The author starts from the classic interpretation of synchronization for synchronous generators and power electronic converters, considered as micro-generators, specifies their mathematical and numerical models and then performs simulation tests. Selected synchronization algorithms are described in detail. Simulation tests are used for analysis of the elaboration of outcomes. The results of simulation tests are handled to formulate a uniform interpretation of synchronization for the micro-generation systems considered. Based on the results obtained, appropriate parallels are built between the two systems being compared. It is shown that the synchronization processes are identical regardless of the micro-generation unit considered. Nonetheless, they differ significantly due to their properties in transient states. Inverter systems have higher dynamics but their disadvantage lies in the relatively high sensitivity to disturbances and the complex selection process of the synchronization algorithm.

Key words: synchronization, micro-generators, SRF PLL, synchronous micro-generator, PV micro-generator.

1. Introduction

Correct synchronization of electric micro-generators with power grids is a key issue increasing power quality and grid stability [1, 6, 11]. Proper synchronization increases the converter's ability to withstand a variety of disturbances occurring in the power system, and thus stabilizes the entire system, especially during fault ride through operation [1, 25, 40]. The above is essential in the currently emerging power grid landscape, where the distributed generation systems are often dominant in the total energy balance. For micro-generators this results in the need to participate actively in the production of electricity and to maintain the power quality imposed by the local grid codes.

The problem of grid synchronization is elaborated herein based on the example of selected distributed micro-generator systems, i.e. hydroelectric (HE) and photovoltaic (PV) power plants connected to the utility grid. These micro-generators represent two distinctively different types of energy sources. A hydroelectric power plant can be classified as a so-called classic generation system, in which electric energy is generated by a three-phase rotating synchronous machine. A photovoltaic micro-generator is connected to the electricity grid via static power electronic converters. Both generators must be accord-

ingly synchronized with the power grid. Conditions for their synchronization are widely described in the literature [6, 11, 31, 33]. This applies, in particular, to synchronous generators that have been in use since the beginning of the development of electricity AC transmission, introduced in late nineteenth century.

According to the state-of-the-art literature [1], when synchronizing any generator with the utility grid, the following conditions must be achieved:

- i. equal rms voltage U_{rms} values of grid and connected generator,
- ii. equal grid and generator frequencies f_{grid}, f_{Gen} ,
- iii. the same phase sequence U_{sec} ,
- iv. equal instantaneous angular phases of synchronized voltage $u_{grid}(t), u_{Gen}(t)$.

After synchronizing a generator with the utility grid, sometimes the above conditions are temporarily violated. This article considers cases of such violations arising on the grid side. Such cases can be caused, for instance, by:

- large voltage variation resulting from symmetrical or asymmetrical sags,
- abrupt changes of the instantaneous synchronization angle resulting from switching operations in the electrical substation,
- presence of nonlinear load generating higher harmonics for the grid.

These examples of disturbances have negative effects on cooperation of micro-generation systems with the utility grid. Due to the necessity of continuous synchronization, the gen-

*e-mail: w.jarzyna@pollub.pl

Manuscript submitted 2019-02-14, revised 2019-04-24 and 2019-06-03, initially accepted for publication 2019-06-03, published in December 2019

eration units react even to temporary disturbances. These may cause significantly different responses of the two generator types being compared herein. This is due to different dynamics and physical properties which keep the generator in synchronous operation.

For example, synchronous generators directly connected to the power grid react spontaneously to voltage disturbances resulting in temporary changes in their power angle. The speed of these changes is usually limited due to significant inertia of the rotating elements and kinetic energy accumulated in these elements. As a result, this action causes a slowdown in the response, which is beneficial when it comes to the suppression of unwanted transient phenomena.

For a photovoltaic micro-generator equipped with a power electronic converter, the effects of disturbances are much more spectacular. These systems are more sensitive to temporary deviations of synchronization conditions for several reasons. The first one is the low value of the electrical energy stored in the capacitors of the DC circuit [2]. Due to this fact, the system cannot compensate for disturbances, which results in a prompt reaction.

In addition, the synchronization process is based on a signal generated by special, complex algorithms [3–6]. There are a few such algorithms that differ in structure, operation principles, immunity to disturbances and speed of operation. These algorithms can be sensitive to specific disturbances, hence choosing them correctly constitutes a very important and even decisive factor in the quality of the synchronization process. The richness of bibliographic sources stands as evidence of the importance of synchronization process. At a number of research centers, these issues were the subject of scientific publications. The leading ones include Aalborg University, represented by Frede Blaabjerg and Remus Teodorescu [6–8, 33], and Technical University of Catalonia with Pedro Rodríguez and Alvaro Luna [7–9]. This issue was also addressed by Marian P. Kaźmierkowski, Mariusz Malinowski and Marek Jasiński, from Warsaw University of Technology [10, 11, 40–42] and Dushan Boroyevich from Virginia Polytechnic Institute and State University, Blacksburg VA [4, 12]. Currently, these works are still being developed, and their goals include adaptive algorithms [13–15] or work with frequency synchronization systems [7, 8] that have a special application in islanded grid systems.

Significant achievements in the development of generation systems can also be attributed to Lublin University of Technology, represented by the author. The doctoral dissertation of P. Lipnicki and D. Zieliński, supervised by the author, allowed to systematize this broad subject matter and to develop the authors' own synchronization methods resistant to notch type disturbances [16, 17, 35] or robustness on voltage fluctuations [18, 19, 22]. Moreover, application of the comb and Savitzky-Golay digital filters, proposed in T. Chmielewski's doctoral thesis, provided the opportunity to extend the spectrum of grid-tied converters and to further improve their performance [20, 21].

The idea behind this article is an attempt to propose universal relations between different generation systems represented by conventional synchronous machines, rotating with constant

speed, and grid-tied power electronic converters, coupling micro-sources of varying power parameters with a power grid. Despite their different structures and different principles of operation, the author points out a common concept of synchronization. This concept is studied on the example of micro-generation systems of similar nominal powers.

The category of micro-generation systems with synchronous generators can be exemplified by hydroelectric or diesel generators, while systems with power electronic converters can be represented by photovoltaic generators, wind power plants as well as electrochemical or flywheel energy storage. In this survey, both groups are represented, respectively, by a hydroelectric plant with an externally excited synchronous generator and by a photovoltaic generator with a grid-tied power electronic converter.

In Section 2 the initial stage for the analysis is set up by means of synchronization rules specified for synchronous generators. These rules are then transferred to power electronic converters and, as a consequence, they differ only in the manner of implementation, caused by completely different structure and principle of operation. Algorithmically they are represented by the synchronization angle, which is formed as a sawtooth trace for the ideal sinusoidal voltage condition, regardless of the type of the micro-generation system applied.

In Section 3 detailed structures of micro-generation systems are defined. Moreover, an interpretation of power angle changes during voltage sags is shown for an HE power plant. A diagram of the PV generator system and examples of synchronization algorithms are presented.

A presentation follows the results of selected disturbance studies and interpretation of this research. Differences and common features of the synchronization processes are discussed. Conclusions are formulated, indicating advantages and disadvantages of both groups.

2. Analysis of instantaneous synchronization angles

During synchronization, the first three conditions i–iii are checked with steady-state measurements. The verification of the ivth condition requires the use of the transient state regulation system. The perfect fulfillment of condition iv is the equality of grid and micro-generator instantaneous phase angles, interpreted as synchronization angles.

In a three-phase symmetrical electrical network, the phase voltages have equal amplitudes and are shifted from each other by a $2\pi/3$ radian. Assuming zero initial angles, the voltage equation of the grid is determined by formulas (1).

$$\begin{aligned}
 u_A(t) &= U_{Am} \sin(\omega_g t) \\
 u_B(t) &= U_{Bm} \sin\left(\omega_g t - \frac{2}{3}\pi\right) \\
 u_C(t) &= U_{Cm} \sin\left(\omega_g t - \frac{4}{3}\pi\right)
 \end{aligned} \tag{1}$$

where:

- U_{Km} – is the amplitude of the fundamental harmonics of phase voltages for $K = A, B$ or C ,
- ω_g – is the network angular frequency.

Similarly, voltage synchronized with the micro-generator network is determined as in formulas (2).

$$\begin{aligned} u_{A\mu}(t) &= U_{A\mu m} \cos(\omega_{\mu}t) \\ u_{B\mu}(t) &= U_{B\mu m} \cos\left(\omega_{\mu}t - \frac{2}{3}\pi\right) \\ u_{C\mu}(t) &= U_{C\mu m} \cos\left(\omega_{\mu}t - \frac{4}{3}\pi\right) \end{aligned} \quad (2)$$

where the μ -index stands for micro-generator unit.

The instantaneous variables of the synchronization angles $\theta_g(t)$ and $\theta_{\mu}(t)$ for phase A are determined by formula (3).

$$\begin{aligned} \theta_g(t) &= \int_0^{\tau} \omega_g dt \\ \theta_{\mu}(t) &= \int_0^{\tau} \omega_{g\mu} dt + \delta \end{aligned} \quad (3)$$

- where τ – operation time,
- δ – synchronization shift angle caused by external disturbances.

The traces of the grid $\theta_g(t)$ and micro-grid $\theta_{\mu}(t)$ phase angles obtained for constant grid frequency (line 1), variable micro-grid frequency (2, 4) and random synchronization shift angle (2) are presented in Fig. 1.

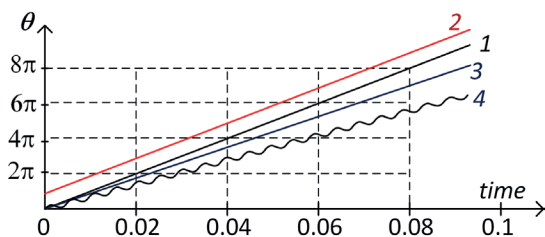


Fig. 1. Examples of instantaneous phase angles of: 1 – $\theta_g(t)$ of the utility grid, 2 – micro-grid with constant synchronization shift angle, 3 – micro-grid with lower frequency, 4 – micro-grid with lower fundamental frequency and higher harmonics

In the expressions of equations (1) and (2), the phase angles are arguments of cosine trigonometric functions, hence instead of presenting them with the infinite line, like in Fig. 1, it is possible to interpret them in 2π intervals. Thus, the linearly dependent phase angle (line 1) is realized as a sawtooth relation $\theta_g(t)$ in Fig. 2. Therefore, in order to fulfill the condition of perfect synchronization of sinusoidal voltages, it is sufficient for sawtooth traces $\theta_g(t)$ and $\theta_{\mu}(t)$ to overlap.

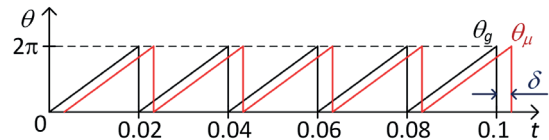


Fig. 2. Requirement for identical sawtooth functions of the collaborating generator systems, where $\theta_g(t)$ (black line) represents the sawtooth angle of the utility grid, $\theta_{\mu}(t)$ (red line) – the synchronized micro-grid, δ – the difference in the synchronization angles which should be close to zero during synchronization

In the further part of the article, sawtooth relations are defined as synchronization functions. Generating these functions for each phase applies only in special cases.

During the synchronization of a micro-generator with the utility grid, it is necessary to equalize the instantaneous phase angle of micro-grid $\theta_{\mu}(t)$ with the phase grid angle $\theta_g(t)$. If these phase angles are not identical and their traces do not overlap, the difference between these angles $\delta(t)$ is a measure of the transient phase shift of the synchronized micro-generator and is defined by relation (4).

$$\theta_g(t) - \theta_{\mu}(t) = \delta(t) \quad (4)$$

Essentially, they are defined for the representation of all phases that can take into account sine wave deformation and asymmetry. Such a representation for instantaneous values is expressed by the transformation to the so-called spatial vector conversion. Mathematically, such an image can be obtained by means of transformation into spatial vector $[1 \ a \ a^2]$, where $a = \exp(j2\pi/3)$ [23–25], or in an equivalent manner in a matrix equation defined as the Clarke $T_{\alpha\beta}$ transformation (5) [26].

$$\mathbf{U}_{\alpha\beta} = \begin{bmatrix} U_{\alpha} \\ U_{\beta} \end{bmatrix} = \mathbf{T}_{\alpha\beta} \mathbf{U}_{abc} = \frac{2}{3} \begin{bmatrix} 1 & -\frac{1}{2} & -\frac{1}{2} \\ 0 & \frac{\sqrt{3}}{2} & -\frac{\sqrt{3}}{2} \\ \frac{1}{2} & \frac{1}{2} & \frac{1}{2} \end{bmatrix} \begin{bmatrix} U_a \\ U_b \\ U_c \end{bmatrix} \quad (5)$$

As a result of these transformations, the voltage vector $\mathbf{U}_{\alpha\beta}$ is determined in a stationary $\alpha\beta$ frame. For sinusoidal and symmetrical \mathbf{U}_{abc} voltages the $\mathbf{U}_{\alpha\beta}$ vector rotates at a constant angular speed determined by grid frequency ω_g . The coordinate system in which this vector is described is the stationary system $\alpha\beta$, corresponding to the coordinate system of complex variables Re-Im.

The $\mathbf{U}_{\alpha\beta}$ vector is represented by two orthogonal components U_{α} and U_{β} which, like the phase voltages, are sinusoidal variables. Therefore, phase angle $\theta_g(t)$ varies proportionally and for constant voltage frequency, its amount is a product of angular frequency and time to $\theta_g(t) = \omega_g t$. Thus, synchronization function of the \mathbf{U}_{abc} vector corresponds to the $U_{\beta}(t)$ voltage component (Fig. 3).

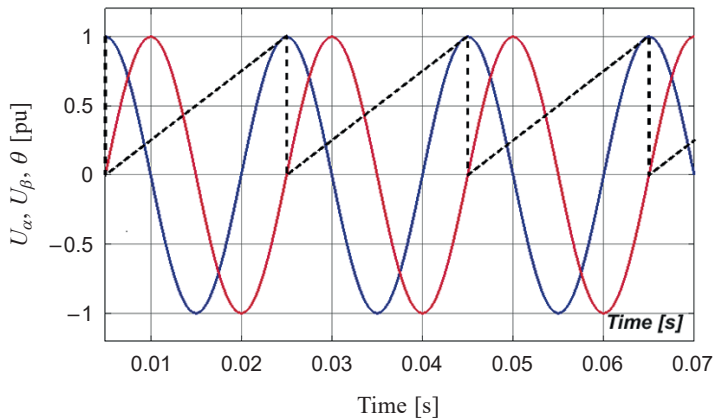


Fig. 3. Components of the complex voltage vector $U_{\alpha\beta}$, where U_{α} – blue line, U_{β} – red line, and the sawtooth synchronization angle θ_g – dashed line

For deformed U_{abc} voltages, e.g. those disturbed by higher harmonics, or in the case of a two-phase short circuit, the synchronization angle $\theta_g(t)$ loses the sawtooth shape [26]. Exemplary interpretations of the $\theta_g(t)$ angle for the voltage disturbed by the fifth harmonic and for the two-phase supply voltage set are shown in (Fig. 4).

The impact of certain disturbances on the synchronization process of the electromechanical hybrid energy system with a synchronous generator and a PV generator with power electronic inverter are the subject of subsequent parts of the article.

3. Impact of certain disturbances on synchronization of micro-generators with the power grid

During the operation of micro-generation systems with the power grid, various disturbances may occur, causing adverse synchronization conditions and negatively affecting the synchronization angle, phase currents and oscillations of instantaneous power p and q . Examples of these disturbances include:

- step change of the synchronization angle,
- symmetrical and asymmetrical voltage sags,
- higher harmonics interferences.

The disturbances mentioned above affect particularly adversely the operation of power electronic micro-generation systems. This is primarily related to the high dynamics of power electronic systems.

To illustrate such events, simulation tests were carried out for two micro-generation systems with equal nominal power of 10 kVA. The first unit is a hydroelectricity plant with an external excitation synchronous generator (HE) directly connected to power terminals. The second one is a photovoltaic stack coupled with the power grid through a power electronic inverter. Due to the demand for dynamic control, the inverter is a vector control system with voltage oriented control (VOC) employed.

The operation of each of the micro-generators studied was simulated using Matlab/Simulink software. Both the HE and

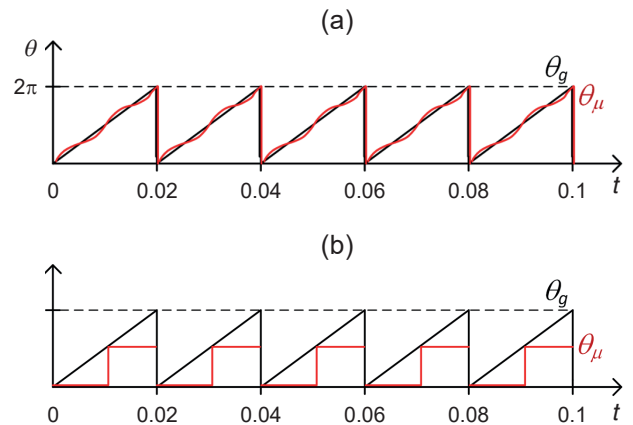


Fig. 4. Sawtooth synchronization graphs (black lines) at ideal U_{abc} voltages and deformed graphs (red lines): a) disturbed by higher harmonic, b) at a single-phase power supply

PV systems were connected to the point of common coupling (PCC) of the power grid. During the simulations, the influence of disturbances on the synchronization process was observed.

3.1. Operation of hydroelectric generator during grid disturbances.

It was assumed that the main components of the water micro-generator system taken into consideration are the Francis turbine, the synchronous generator with electromagnetic excitation, the excitation control system and the speed power governor system (Fig. 5). The water flow is controlled by means of guide vanes adjusting the turbine load. The guide vanes consist of a number of blades that can be adjusted in order to increase or reduce the flow rate through the turbine. The speed-power governing system of the turbine adjusts the turbine-generator speed based on the feedback signals of deviations of both the grid frequency and micro-generator with respect to their reference settings [44–46].

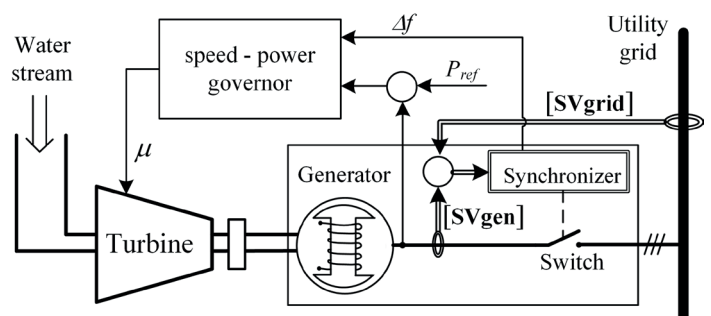


Fig. 5. Simplified diagram of a hydroelectric plant with an external excitation synchronous generator, speed-power governor adjusting the position of guide vanes (μ), and a synchronizer checking the synchronizing conditions based on delivered synchronization vectors SV_{grid} and SV_{Gen} . A synchronizer is a control system performing automatic synchronization with equalization of voltages and frequencies along with switch closure when all the synchronization conditions are simultaneously met

A synchronizer checks the conditions delivered by the vectors:

$$\begin{aligned} \mathbf{SV}_{\text{grid}} &= [U_{\text{rms-grid}}, f_{\text{grid}}, U_{\text{sec-grid}}, u_{\text{grid}}(t)], \\ \mathbf{SV}_{\text{Gen}} &= [U_{\text{rms-Gen}}, f_{\text{Gen}}, U_{\text{sec-Gen}}, u_{\text{Gen}}(t)], \end{aligned}$$

and after their fulfillment it closes a switch.

For the adopted scope of the research, a mathematical model of the generator is formulated using equations of the synchronous machine in a transient state [28]. The mechanical side of a turbine is represented by a first-order inertia system, and the speed control system is approximated by a master loop feedback with a proportional controller. This is determined by the swing equation (6).

$$J \frac{d\omega_m}{dt} = T_m(t) - T_e(t) \quad (6)$$

After multiplication by angular velocity ω_m and having in mind that $\omega_e = \omega_m p$, where p is the number of electric generator pole pairs, we receive:

$$J\omega_m \frac{d\omega_m}{dt} = \omega_m T_m(t) - \frac{\omega_e}{p} T_e(t) \quad (7)$$

where:

T_m – is a mechanical torque delivered to the generator by the turbine,

J, L_m – the moment of inertia of the electromechanical system (J) and angular momentum ($L_m = J\omega_m$),

$$L_m \frac{d\omega_m}{dt} = P_m(t) - P_e(t). \quad (8)$$

The expression for the instantaneous value of the electromagnetic power (9) is determined on the basis of the external excitation synchronous machine model in transient states and a constant rotor flux represented by field components Ψ_d and Ψ_q in a rotating dq reference frame [28].

$$P_e = \frac{3}{2} \omega_m (\Psi_d i_q - \Psi_q i_d) \quad (9)$$

where:

Ψ_d, Ψ_q – are components of the spatial flux vector in a synchronously rotating reference system (after the Park transformation),

i_q, i_d – components of the spatial current vector in a synchronously rotating reference frame.

In order to analyze the behavior of the micro-generator, an interpretation based on a quasi-stationary model (10) is applied, where generated power depends on the product of the grid and micro-grid voltage as well as the sine of the δ_p power angle.

$$P_e = \frac{3U_g U_{\mu g}}{X_g} \sin \delta_p \quad (10)$$

where:

$U_{\mu g}, U_g$ – rms value at micro-generator terminals and at a grid PCC, respectively,
 X_g – grid reactance between the PCC and micro-generator terminals,
 δ_p – power angle.

According to this dependence, the average value of the generated power can be approximated by a sinusoidal function with amplitude P_m . In the event of a voltage sag, this amplitude will decrease in proportion to the sag depth and as a result of this sag the point of operation (P_o, δ_{p_o}) moves initially to (P_1, δ_{p_o}), and after a time depending on the system parameters, the steady state operation will be fixed at a new point (P_o, δ_{p_o1}). Interpretation of changes in the operation point and the accompanying speed changes are shown in Fig. 6.

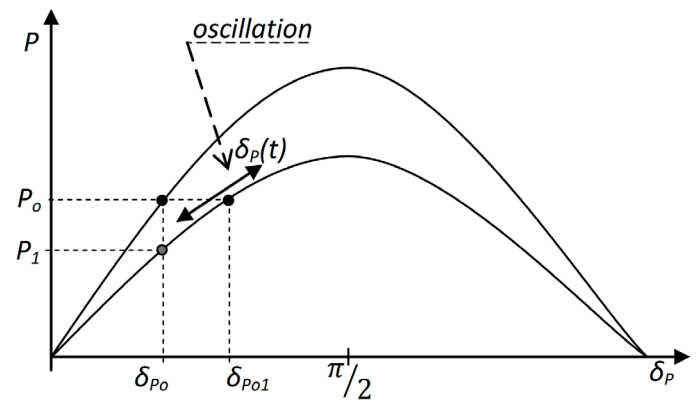


Fig. 6. Changing the operating point during voltage sags causes pulsation of the power angle δ_p , which in turn produces micro-variations of synchronization angle θ_μ

It is evident that changes in the power angle $\delta_p(t)$ also affect the angle of synchronization. Its transient states and oscillations are responsible for the deformations of the saw-tooth shape of the synchronization angle. This phenomenon is easily seen in Fig. 6.

Due to the movement of the operating point, temporary speed changes occur, hence the synchronization angle function is a composition of the described situation (11).

$$\theta_\mu(t) = \int_0^{f^{-1}} \left(\omega_g + \frac{d\delta_p(t)}{dt} \right) dt \quad (11)$$

where f is a grid frequency.

According to the swing equation (6), the speed of change of the operating point depends on the inertia of the system, which is a significant value for electromechanical hydropower plant units, hence oscillation of the operating point is visible in the trace of the synchronization angle.

On the basis of the mathematical description used, the simulation model prepared in the Matlab/Simulink software was specified.

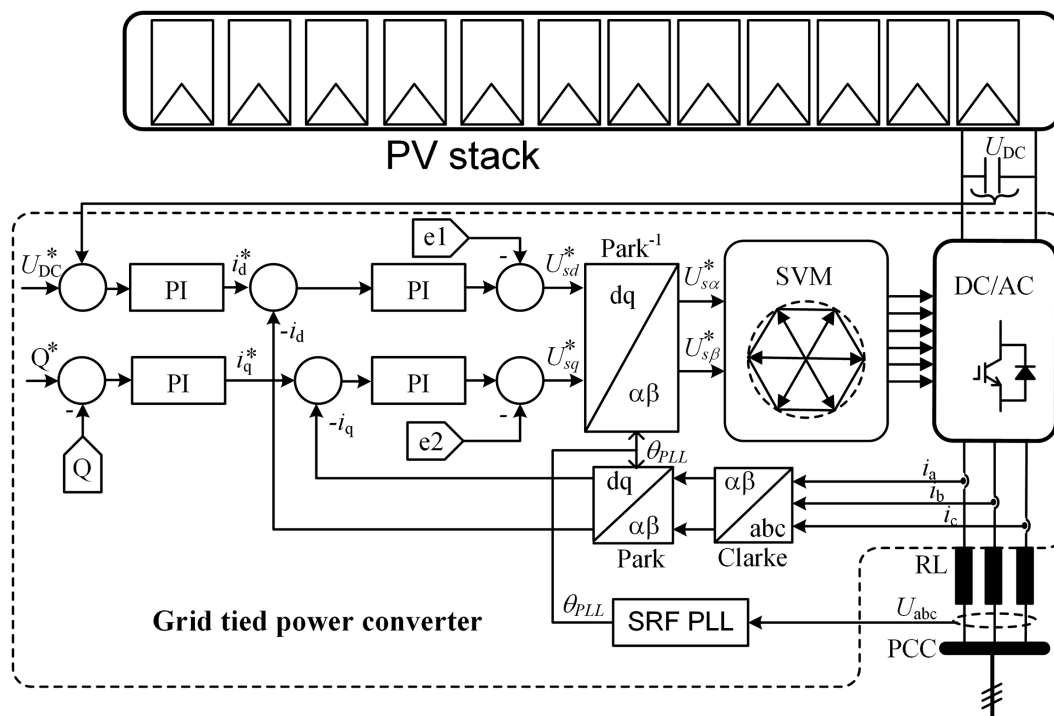


Fig. 7. Diagram of a PV generator synchronized with the utility grid, where $e1 = \omega Li_q + u_d$, $e2 = -\omega Li_d + u_q$

The applied water turbine control system with the master speed controller and direct connection of the synchronous generator to the utility grid causes the rotational speed to only be able to change around the synchronous speed during the occurrence of disturbances on the part of the grid. This behavior takes place until the power on the turbine shaft exceeds the possibility of receiving power by the grid due to a too large voltage sag. Consequently, the rotation increases and the system loses synchronism.

3.2. Structure of the photovoltaic generator. Photovoltaic generators connected to the network are equipped with power electronic inverters. They convert DC voltage into almost sinusoidal voltages with the amplitude and frequency required by the grid. Adjustment of these quantities ensures only the fulfillment of static conditions of integration with the power grid. This converter control is insufficient in grids with high saturation of PV generators because it causes dangerous voltage swells, decreasing voltage quality and reactive power circulations.

To obtain active control of high dynamic properties, it is necessary to apply one of the vector control methods. These control methods are based on transient state models affecting temporary values of amplitude and phase angle [28]. There are two basic methods of regulation applicable to the active operation of grid-tied inverters. These are voltage oriented control (VOC) and direct power control (DPC).

In this paper, the VOC system was applied where feedback control loops with variables responsible for active and reactive power were expressed in the rotating reference frame dq. Therefore, the correct generation of the synchronization signal

is a fundamental task, which is performed by the phase locked loop system (PLL). The diagram of such a generator is shown in Fig. 7.

The inverter applied in PV uses the basic algorithm for synchronization of the three-phase voltages type, i.e. SRF PLL (synchronous reference frame phase locked loop), shown in Fig. 8a [29], where the instantaneous value of the phase angle is detected by means of synchronization of the rotating reference frame with the power grid voltage vector [43].

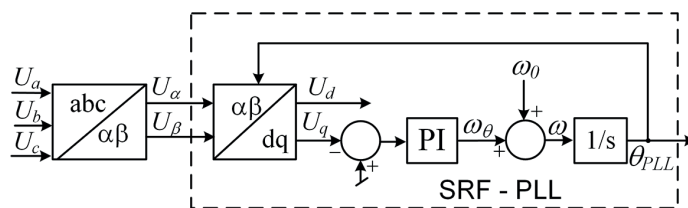


Fig. 8a. Diagram of the synchronous reference frame SRF-PLL algorithm generating a sawtooth synchronization angle

The algorithm uses signals obtained after Clarke transformation which convert a natural abc frame into an $\alpha\beta$ two-phase frame and then Park transformation, converting $\alpha\beta$ into a rotating dq frame. The position of a grid angle is obtained by setting the U_q at zero and then the error is processed by the PI controller. Estimated synchronization angular frequency ω_θ , after adding grid frequency ω_0 and integration of the result, generates the $\theta_{PLL}(t)$ synchronization angle with a grid sawtooth shape for sinusoidal and symmetrical grid voltages.

During high disturbances, the SRF-PLL algorithm does not perform as required in order to ensure high quality of the output power. Hence, other synchronization algorithms can be used which can generate a smooth sawtooth signal in the presence of disturbances. One of the widely applied alternative synchronization algorithms is a double second order generalized integrator (DSOGI) PLL. In the present research, it was used at higher harmonics disturbances.

The DSOGI are the second order resonance filters with an auto tunable structure. In the applied structure (Fig. 8b), such a filter provides positive sequence voltage to SRF-PLL inputs.

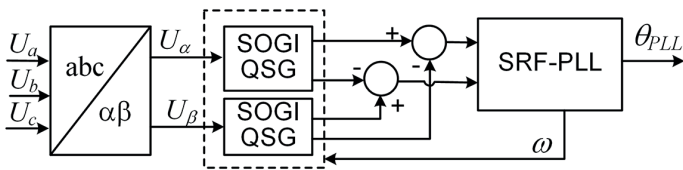


Fig. 8b. Diagram of a double second order generalized integrator DSOGI PLL, where QSG stands for quadrature signal generation

4. Comparative tests for HE and PV generators

Comparative tests were carried out for the described HE and PV generation systems. The responses to exemplary step disturbances were compared:

- Shift of the power grid phase angle,
- Symmetrical voltage sag,
- Asymmetrical voltage sag,
- Abrupt higher harmonics increase.

4.1. Shift of the power grid phase angle. It was assumed that during synchronization of the micro-grid with the utility grid, the difference in the angles of synchronization in accordance with (5) is $\delta = 3\% \cdot 2\pi = 0.188$ [rad]. The tests were conducted for the HE micro-generator and then for the PV. The results obtained are illustrated in the diagrams of Fig. 9a÷d and, respectively, present the results of:

- Voltage output of the micro-generator during its switch-on to the power grid,
- Current output of the HE micro-generator,
- Current output of the PV micro-generator,
- Derivative of synchronization angle of the HE micro-generator,
- Derivative of synchronization angle of the PV micro-generator,
- Instantaneous power pq of the HE micro-generator,
- Instantaneous power pq of the PV micro-generator.

The waveforms presented in the diagrams start from a steady state operation close to the nominal load. Then, due to the switching processes in the power grid, the phase of this grid is shifted by a δ angle. This sudden disturbance causes significant changes in the observed variables, as shown in Figs 9c1÷9d2. In the case of a step shift of the power grid phase angle (Fig. 9a), the current rises (Fig. 9b1) to an alarming value and then falls

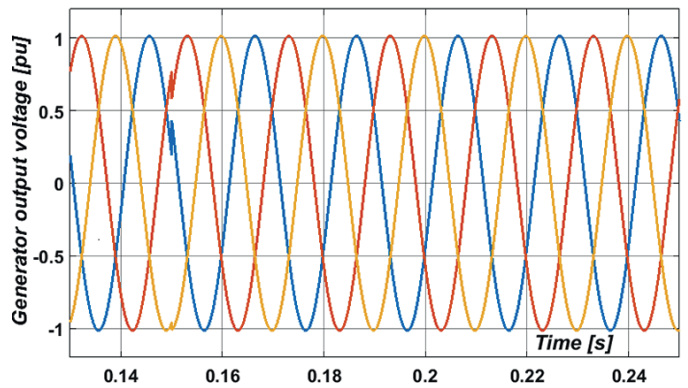


Fig. 9a. Voltage at micro-generator terminals at switching on with a δ difference of the synchronization angles between the voltage of the utility grid and the micro-generator voltage. The disturbance was generated at $t = 0.15$ s

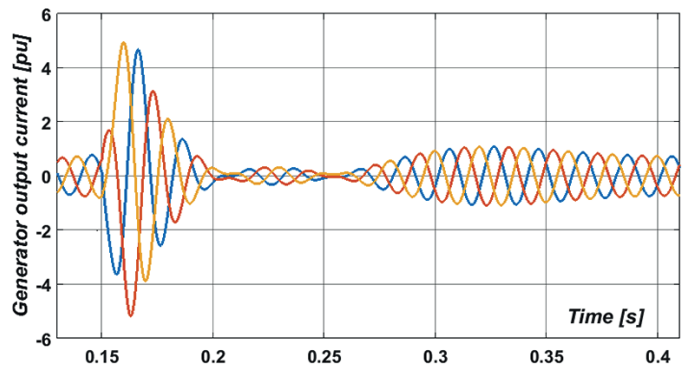


Fig. 9b1. Current output of the HE micro-generator at switching on with a difference of synchronization angles between the utility grid and the micro-generator

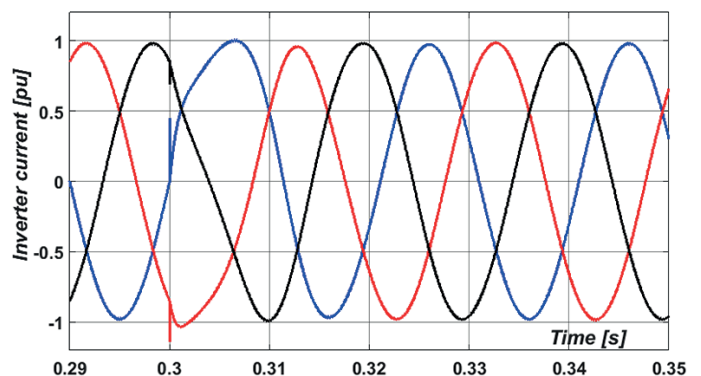


Fig. 9b2. Current output of PV micro-generator at switching on with a difference of synchronization angles between the utility grid and the micro-generator

back to the value determined by the load. The steepness of the current changes depending on the moment of inertia and is determined by the electromechanical time constant of the generator and the gain factor in the speed feedback loop. It should be noted here that a high rate of speed gain can reduce the time

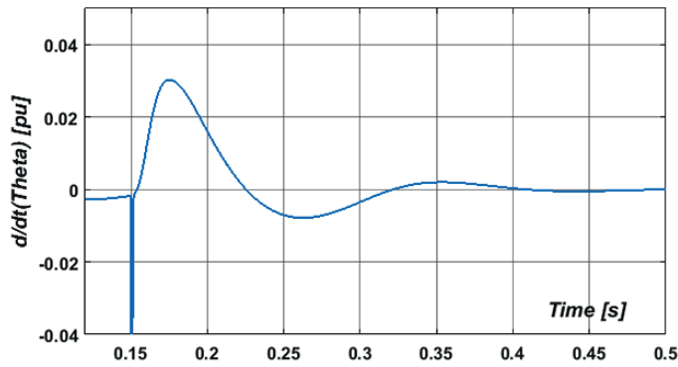


Fig. 9c1. Trace of derivative of the synchronization angle in the HE micro-generator at switching on, caused by a step shift of the power grid phase angle

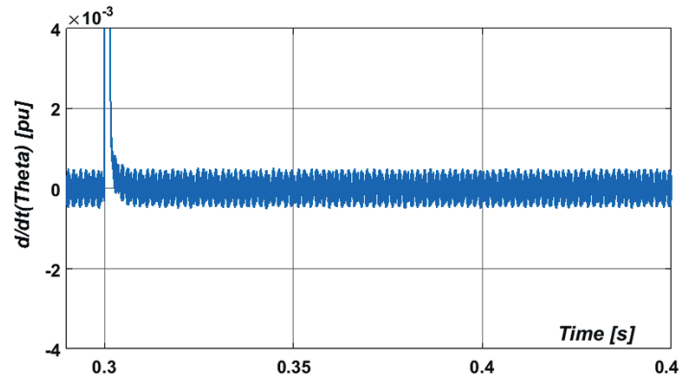


Fig. 9c2. Trace of derivative of synchronization angle of PV micro-generator at switching on, caused by a step shift of the power grid phase angle

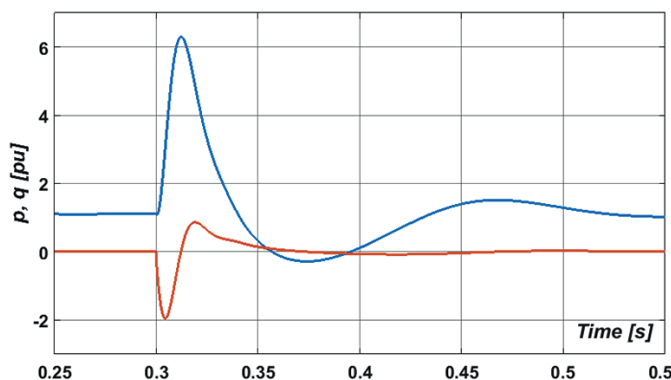


Fig. 9d1. Instantaneous power pq characteristics of HE micro-generator at switching on, caused by a step shift of the power grid phase angle

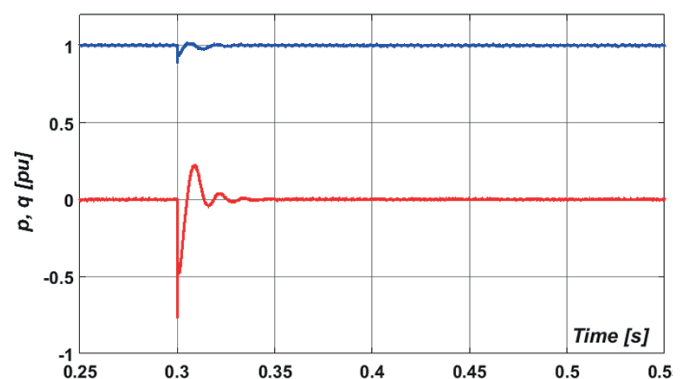


Fig. 9d2. Instantaneous power pq characteristics of PV micro-generator at switching on, caused by a step shift of the power grid phase angle

constant; on the other hand, it can cause unwanted oscillations in reaching the target value.

For the same disturbances, the current output of the PV micro-generator was significantly different. Due to the high speed of control, the current changes were practically unnoticeable.

The outputs of other compared variables were also very different. In all transient state cases of the HE micro-generator, the variables were accompanied by long-term oscillations. Except for changes in the synchronization angle (Fig. 9b2), the maximum values of the HE micro-generator also exceeded those that were obtained for the PV micro-generator.

4.2. Symmetrical voltage sag. Voltage sags are disturbances that often happen in the power grid. They are mainly caused by faults on transmission lines, which may be symmetrical, during short-circuiting of three phases, or asymmetrical, e.g. with a two-phase short circuit. The depth of the dip depends on the location of the fault and fault resistance.

In this paper, the topic of voltage sags is described in two subchapters. The current subchapter analyzes symmetrical sags and the next one – asymmetrical ones.

It was assumed that the voltage sag occurs in the power grid in a step way and its depth is about 30% (Fig. 10a). This

voltage change causes variation of synchronization states. In the synchronous generator, the power angle δ adjusts to current conditions and in the case of power electronics inverters, the voltage vector $U_{\alpha\beta}$ can be modified.

During the experiments, similarly to the previous studies, currents (Fig. 10b2) derivative of the synchronization angle (Fig. 10c1, Fig. 10c2) and instantaneous power pq (Fig. 10d1,

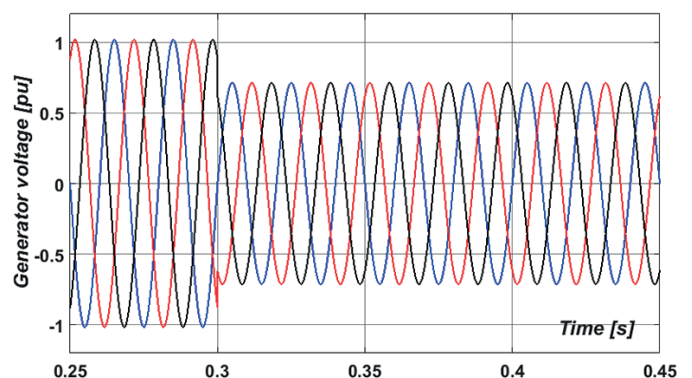


Fig. 10a. Voltage sag of a 30% symmetrical decrease due to a three-phase short circuit

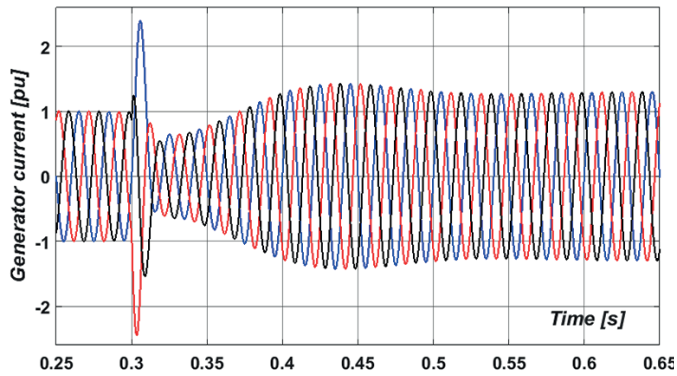


Fig. 10b1. Current output of the HE micro-generator after a symmetrical sag

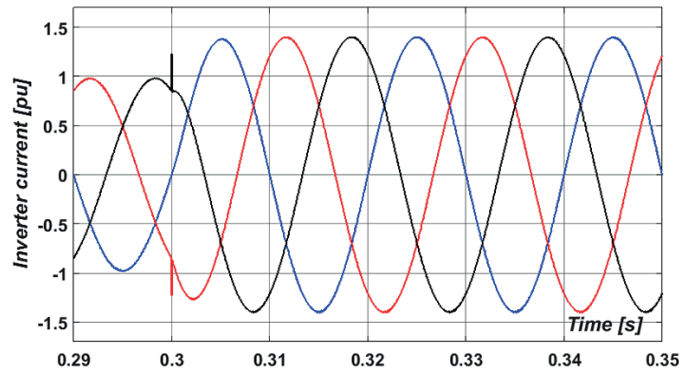


Fig. 10b2. Current output of the PV micro-generator after a symmetrical sag

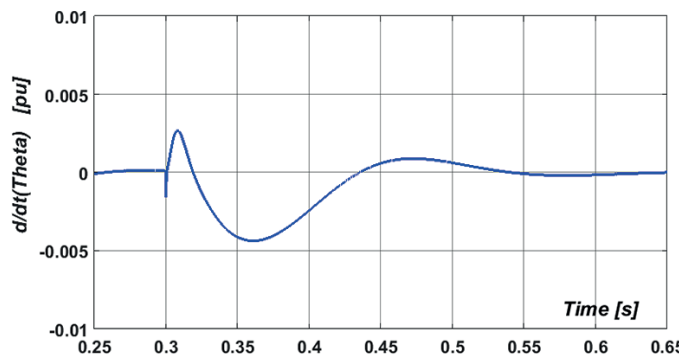


Fig. 10c1. Trace of derivative of the synchronization angle of the HE micro-generator caused by a symmetrical voltage sag

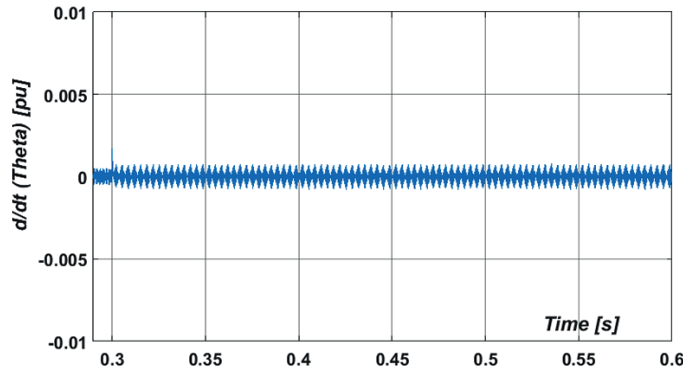


Fig. 10c2. Trace of derivative of the synchronization angle of the PV micro-generator, caused by a symmetrical voltage sag

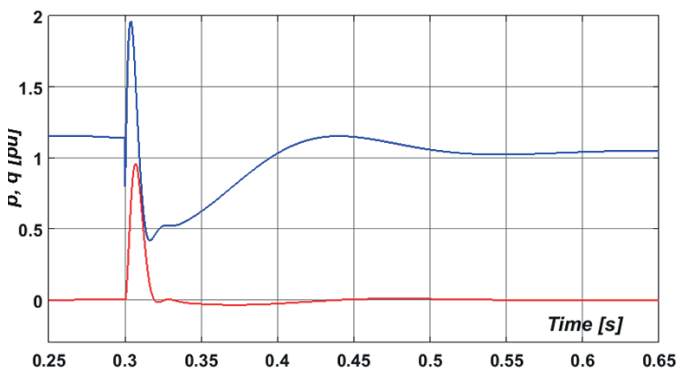


Fig. 10d1. Instantaneous power pq characteristics of the HE micro-generator caused by a symmetrical voltage sag

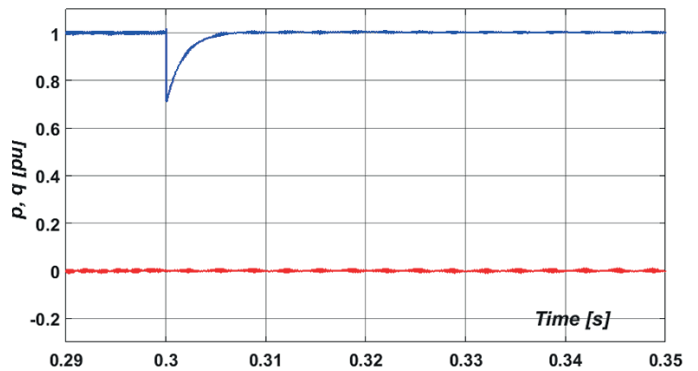


Fig. 10d2. Instantaneous power pq characteristics of the PV micro-generator caused by a symmetrical voltage sag

Fig. 10d2) were tested. The results obtained for both the micro-generators were compared and considered.

The voltage sag due to the symmetrical short-circuit results in a rapid increase in the current, whose fixed value depends on the network parameters. This is also accompanied by transient states, particularly pronounced for the HE micro-generation system.

As it transpires from analyzing the results presented throughout Fig. 10, smaller overshoots after the symmetrical sag occurrence are created in the PV micro-generator. The HE micro-generator responds with greater amplitude of a tran-

sient state because during the sag the operating point (Fig. 6) is changed. Stabilization in a new position takes some time depending on the HE inertia.

The power electronics converter response varies significantly from the HE unit behavior. The amplitudes of the observed variables are visibly smaller. This can be explained by the fact that during the symmetrical sag only the amplitude of the $U_{\alpha\beta}$ vector of voltage changes while the phase of $U_{\alpha\beta}$ remains unchanged. Thus, the current increases up to the value which compensates for the voltage decrease while the power after a short transient state comes back to the reference value.

On the basis of the results obtained, it can be stated that the PLL synchronization algorithm is very robust at symmetrical voltage sags.

4.3. Asymmetrical voltage sag. Asymmetrical sags are more challenging than the symmetrical ones analyzed in the previous subsection. Similarly as in the previous tests, the sag level in the two faulty phases reached 30% (Fig. 11a).

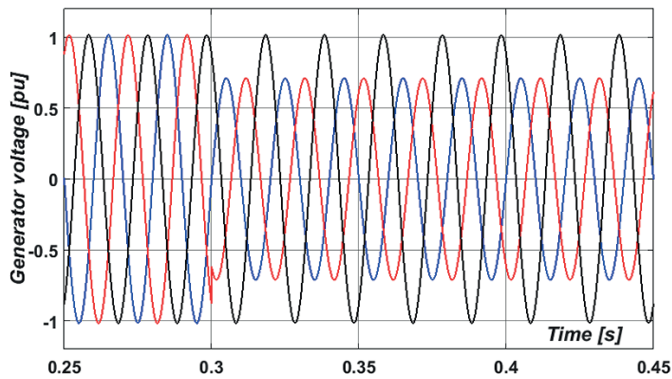


Fig. 11a. Asymmetrical 30% voltage sag caused by a two-phase short circuit

During these tests, the currents of two shorted phases almost overlapped with each other (Fig. 11b1). Such a current shape is a result of shortage of two phases which causes the $U_{\alpha\beta}$ vector to mostly pulsate instead of rotating. Such relationships may cause significant overloads and dangerous pulsations.

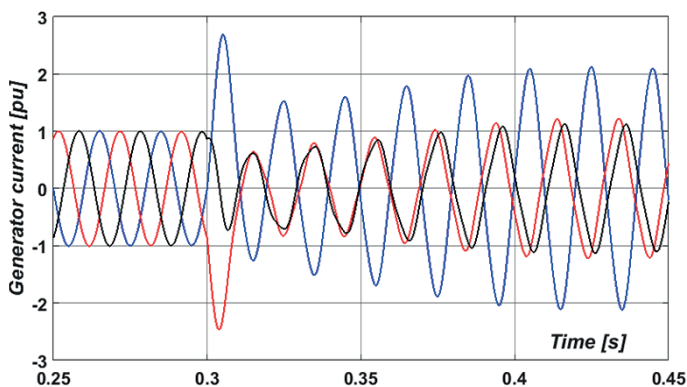


Fig. 11b1. Current response at an asymmetrical 30% voltage sag of the HE micro-generator

An asymmetrical voltage sag creates much more difficult operating conditions for the generator than a symmetrical one. For the HE micro-generator, currents have larger asymmetry in terms of amplitude (Fig. 11b1). In one phase, a short-circuit amounts to almost double the nominal value. However, for PV micro-generators, thanks to the efficient reaction of the control system, the amplitudes of the currents in all phases are similar,

and their values are limited to the value allowed by the control system (Fig. 11b2).

An interesting fact is that the changes of synchronous angle are almost identical for both micro-generators (Fig. 11c1 and Fig. 11c2). In both systems, this angle oscillates at around 100 Hz and their amplitude is around 1000 times greater than during the symmetrical voltage sag.

The instantaneous powers p and q also oscillate at around 100 Hz. For the PV micro-generator, the amplitude of oscillations is significantly smaller than for the HE one.

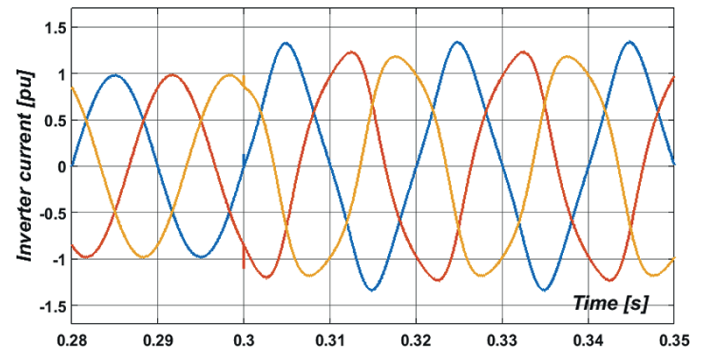


Fig. 11b2. Current response at an asymmetrical 30% voltage sag of the PV micro-generator

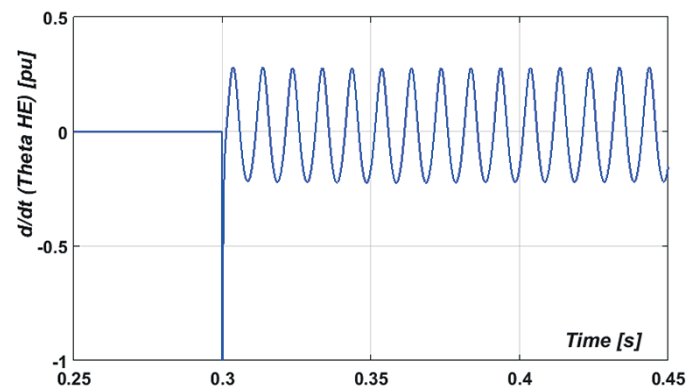


Fig. 11c1. Trace of derivative of the synchronization angle of the HE micro-generator caused by an asymmetrical voltage sag

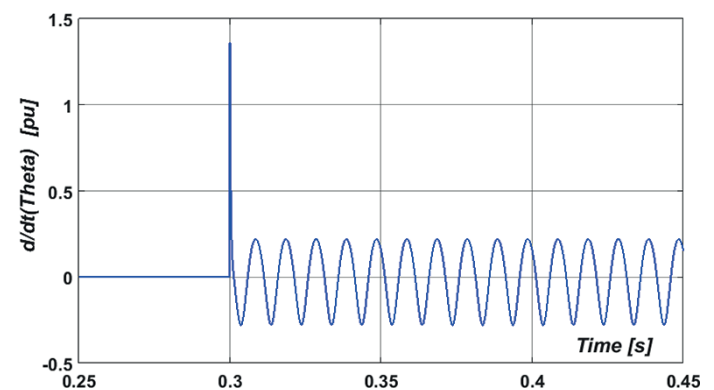


Fig. 11c2. Trace of derivative of the synchronization angle of the PV micro-generator caused by an asymmetrical voltage sag

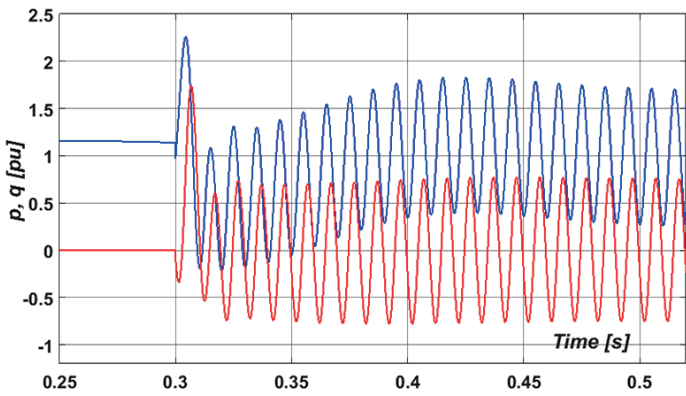


Fig. 11d1. Instantaneous power pq characteristics of the HE micro-generator caused by an asymmetrical voltage sag

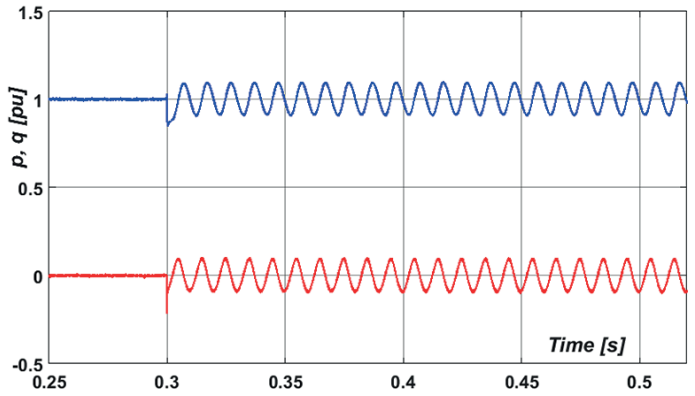


Fig. 11d2. Instantaneous power pq characteristics of the PV micro-generator caused by an asymmetrical voltage sag

The above reaction could be predicted. Dual power frequency pulsations are characteristic of two-phase short circuits. The micro-generator with such a reaction actively participates in the reconstruction of the mains voltage. From the point of view of the fault ride through (FRT) requirements and grid strength, this is a desirable reaction.

The PV micro-generator with the inverter and applied SRF-PLL algorithm can reduce these vibrations and even completely eliminate them. Such an effect can be obtained when the synchronization algorithm designated in Fig. 7 estimates the synchronization angle corresponding to the distorted network voltage [29]. In the discussed case of the two-phase short-circuit, the synchronization signal should be of a rectangular shape, as in Fig. 4b. The possibility of such an action is a significant benefit indicating an important feature of micro-generators which fulfil the FRT requirements but do not strengthen a faulty grid. Instead, the inverter adapts itself to faulty conditions and can, therefore, minimize currents and the instantaneous pq power.

4.4. Influence of higher harmonics on grid synchronization.

Higher harmonics are generated by various nonlinear loads. Their presence affects the efficiency of devices supplied from such a polluted utility grid in a negative manner, and may pose

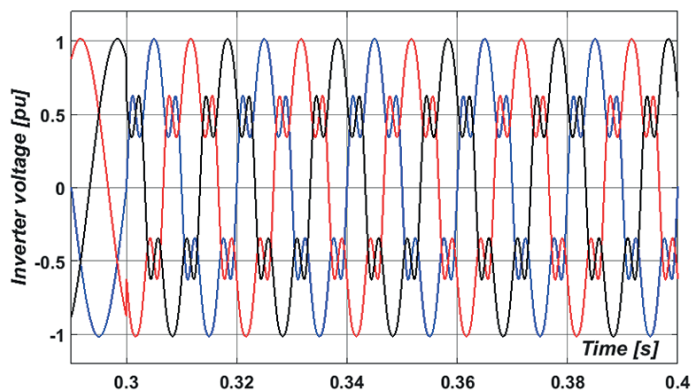


Fig. 12a. Characteristics of grid voltage deformed by higher harmonics of 5th and 7th order and THDu = 20%

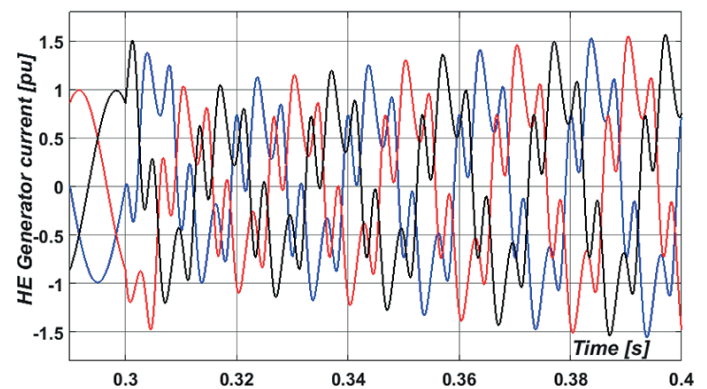


Fig. 12b1. Current characteristics of the HE micro-generator with higher harmonics distortion of 5th and 7th order and THDu = 20%

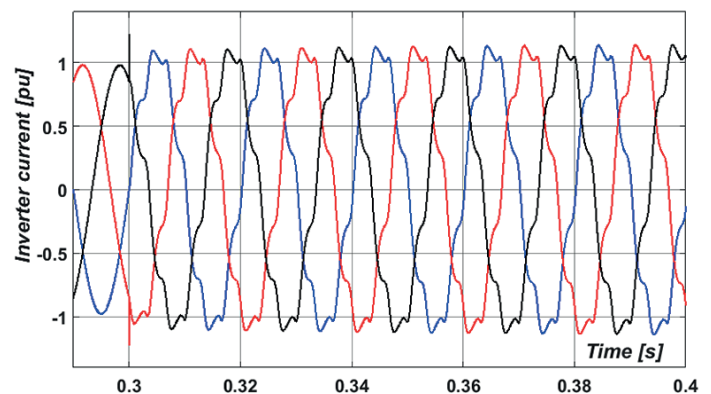


Fig. 12b2. Current characteristics of the PV micro-generator current with strong higher harmonics distortion of 5th and 7th order and THDu = 20%

a serious risk for micro-generation systems connected to the grid. In the current tests, distortions of 5th and 7th order harmonics have been introduced to the utility grid at THD level of 20%.

For the utility grid with higher harmonics, instantaneous currents as well as currents in steady states are much higher

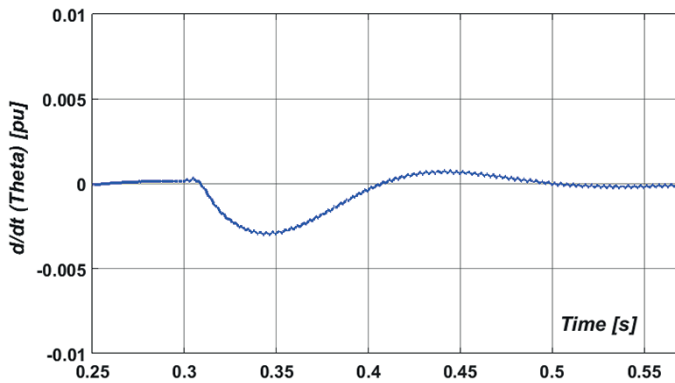


Fig. 12c1. Trace of derivative of the synchronization angle of the HE micro-generator with strong higher harmonics distortion of 5th and 7th order and THDu = 20%

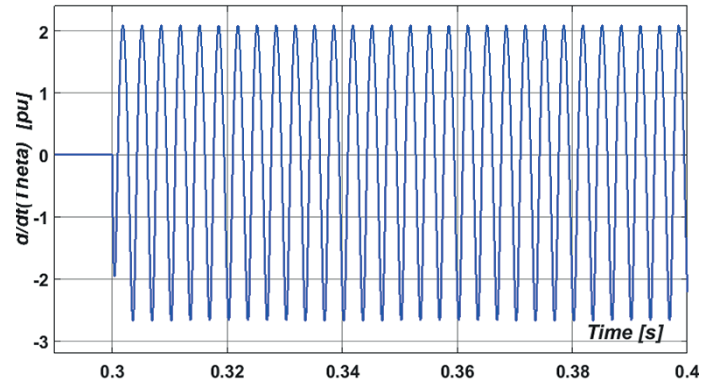


Fig. 12c2. Trace of derivative of the synchronization angle of the PV micro-generator synchronized by the PLL-SRF algorithm, with strong higher harmonics distortion of 5th and 7th order and THDu = 20%

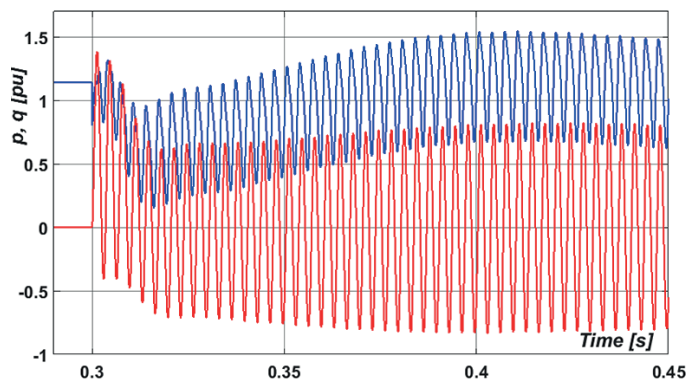


Fig. 12d1. Instantaneous pq power characteristics of the HE micro-generator with strong higher harmonics distortion of the power grid

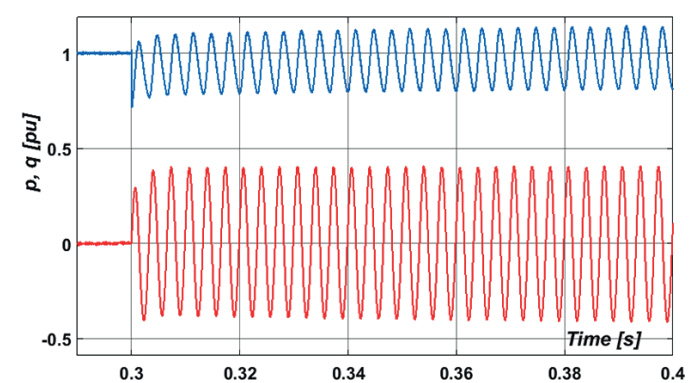


Fig. 12d2. Instantaneous pq power characteristics of the PV micro-generator operating under the PLL-SRF synchronization algorithm

for the synchronous generator than for the PV power electronic inverter. This is due to the fact that the HE micro-generator system outputs sinusoidal voltage. This causes significant instantaneous voltage difference between grid and micro-grid voltage and therefore currents and their THDu significantly increase.

In the case of the PV micro-generator with an inverter synchronized by SRF-PLL, the synchronization angle changes similarly to that depicted in Fig. 4. Hence, the voltage produced is also distorted. For this reason, phase voltage drops are smaller than in the case of the HE micro-generator. Moreover, phase currents have much lower amplitude values and lower THDu values than in the HE micro-generator.

Taking account of the previous reasoning, it is easy to explain the characteristics in Fig. 12c1 and Fig. 12c2. The amplitude of $d\theta/dt$ is negligibly small. Moreover, despite the time right after the introduction of the higher harmonics, the phase angle of the HE micro-generator increases linearly. The situation is completely different for the PV micro-generator with the SRF-PLL synchronization algorithm. Because this algorithm is not resistant to higher harmonics, the higher harmonics distortions introduced are extended to the synchronization angle θ and in consequence to the synchronization angle changes shown in Fig. 12c2.

For the same reasons, instantaneous pq power has higher amplitudes for HE than for the PV micro-generator. The relevant characteristics are shown in Fig. 12d1 and Fig. 12d2.

The results presented do not include all the characteristics of PV micro-generators equipped with vector-controlled inverters. These characteristics can be formulated according to specific requirements. We can influence the features of the system by selecting the synchronization algorithms, introduce extended control systems as well as changes in topology.

Examples of these properties are shown for the last tests. They are repeated for the PV micro-generator with the synchronization algorithm which is resistant to higher harmonics distortion. Based on references [6, 7, 30, 31], the double second order generalized integrator PLL (DSOGI-PLL) algorithm was chosen. To present the influence of this algorithm on synchronization of the characteristics, the trace of the derivative of the synchronization angle and instantaneous pq power characteristics of the PV micro-generator are shown in Fig. 12c3 and Fig. 12d3.

Significant stabilization of the synchronization angle was obtained for the DSOGI algorithm [10, 11, 30–32]. Therefore, an inverter with this algorithm seems to be more resistant to interference from higher harmonics than one with the SRF-PLL algorithm. However, the limitation of these pulsa-

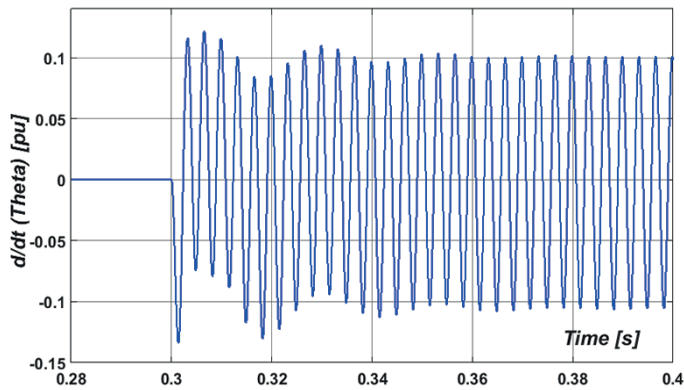


Fig. 12c3. Trace of derivative of the synchronization angle of the PV micro-generator synchronized by the DSOGI-PLL algorithm, with strong higher harmonics distortion of 5th and 7th order and THD = 20%

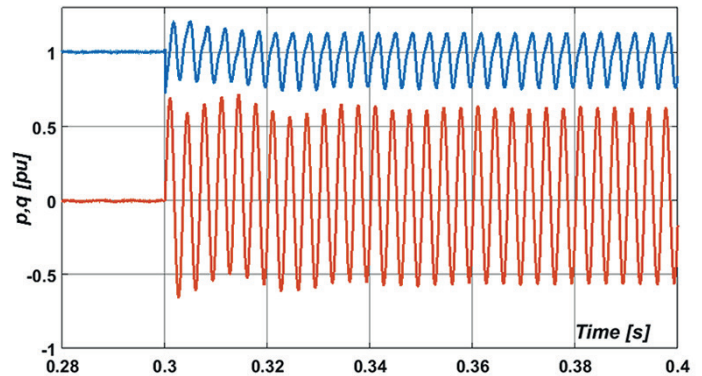


Fig. 12d3. Instantaneous pq power characteristics of the PV micro-generator synchronized by the DSOGI-PLL algorithm, with strong higher harmonics distortion of 5th and 7th order and THD = 20%

tions does not have a significant impact on the instantaneous pq power pulsations. This happens because an inverter with the DSOGI-PLL algorithm generates a nearly sinusoidal voltage, while the utility voltage is strongly disturbed. Therefore, large amplitude pulsations of pq are produced, and their maximum values are comparable to HE micro-generators.

The last experiment with the DSOGI-PLL synchronization algorithm indicates that synchronization procedures should be chosen very carefully, always bearing in mind the nature of the disturbances and the overall control structure.

5. Conclusions

The paper showed that synchronization of synchronous generators and power electronic inverters are equivalent processes. They both enable collaboration of micro-generation systems with the power grid.

In classic synchronous generators, synchronization is a process based on physical phenomena and can be carried out spontaneously. Interference in the synchronization process can take place mainly through turbine control or excitation circuit control systems.

In power electronic inverters, a special synchronization system is required. It usually is implemented as a set of digital algorithms. Just like in a synchronous generator, these algorithms work in online mode, producing a synchronization signal during working time.

Significant differences in operation occur when the grid voltage is disturbed. This results in synchronous generators reaction with long-lasting transient states. Transient values of current and instantaneous pq power are obtained with far greater excesses than those observed in the inverter. This behavior results from the lack of direct fast control circuits for current and instantaneous pq power. Nevertheless, even during different disturbances, synchronous generators always produce sinusoidal voltages according to a symmetrical three-phase system.

Power electronic inverters behave differently. Based on estimated information about the synchronization angle, the

inverters generate voltages corresponding to this synchronization signal. If the signal is distorted, then the voltages will be deformed to the same extent. This can be dangerous to the grid as it will consolidate the incorrect state of the operation. Therefore, synchronization algorithms are required to generate a sawtooth signal regardless of the existing disturbance.

To meet this task, a number of complex algorithms have been developed. They can be grouped, e.g. according to immunity to disturbances. There are also attempts to build multi-variable synchronization control structures [47] and to also build universal algorithms with adaptive structures. However, the main disadvantage of these latter algorithms is their long processing time. The effects of a long delay in dynamic states are dangerous, hence in practical applications, the quick classic SRF-PLL solution is used most frequently.

It is also possible to arbitrarily generate a sawtooth shape and synchronize only in the time periods specified by the zero crossing of the voltage. However, control over what is happening in the grid is lost. This solution can cause high risks in the case of disturbances occurrence. One of such hazards is the erroneous detection of the voltage zero crossing. Such a system loses its synchronization completely, which is consequently equivalent to converter emergency tripping.

In some cases, exceptions from the principles presented herein may exist. Namely, if the power system support is not required in transient states from the converter, then such a converter may generate distorted voltages in a short period of time. Thus, it fits, e.g. into a voltage sag. This action provides relative protection for the inverter from overloading and over-regulation, and limits hazardous instantaneous power flows.

In conclusion, it should be emphasized that the synchronization process plays a fundamental role in the integration of micro-generation systems with the power grid. Power electronic converters are much more powerful in terms of dynamics and optimization of transient states. Their functionality depends, to a large extent, on the synchronization process. That is why there are still a number of issues that require more precise elaboration. A number of scientists are currently working, for example, on adaptive systems [13–15, 31, 34], on the increase of circuit

inertia [2, 36–38] and algorithms designed to work in variable network structures taking account of temporary island work [4, 39]. Further progress in this area should bring benefits, especially in the case of converter systems that operate as dispersed energy sources in networks that perform as smart grids [39, 48].

Acknowledgements. This work was supported under the project “Electric vehicle energy transfer system integrated with lighting infrastructure – PLUGinEV” of the Polish National Centre for Research and Development, project No. POIR.04.01.02–00–0052/16.

REFERENCES

- [1] ENTSO-E Network Code for Requirements for Grid Connection Applicable to all Generators, 26 June 2012, ENTSO-E, Avenue de Cortenberg 100, 1000 Brussels, Belgium.
- [2] M. Ashabani, F.D. Freijedo, S. Golestan, and J.M. Guerrero, “Inductors: PLL-Less Converters with Auto-Synchronization and Emulated Inertia Capability”, *IEEE Transactions on Smart Grid* 7(3), May 2016.
- [3] S. Golestan, J.M. Guerrero, and J.C. Vasquez, “Single-Phase PLLs: A Review of Recent Advances”, *IEEE Transactions on Power Electronics* 32(12), December 2017.
- [4] D. Dong, B. Wen, P. Mattavelli, D. Boroyevich, and Y. Xue, “Modeling and Design of Islanding Detection Using Phase-Locked Loops in Three-Phase Grid-Interface Power Converters”, *IEEE Journal of Emerging and Selected Topics in Power Electronics* 2(4), December 2014.
- [5] D.S. Ochs, B. Mirafzal, and P. Sotoodeh, “A Method of Seamless Transitions Between Grid-Tied and Stand-Alone Modes of Operation for Utility-Interactive Three-Phase Inverters”, *IEEE Transactions on Industry Applications* 50(3), May/June 2014.
- [6] A. Timbus, M. Liserre, R. Teodorescu, and F. Blaabjerg, “Synchronization methods for three phase distributed power generation systems – An overview and evaluation”, *2005 IEEE 36th Power Electronics Specialists Conference*, pp. 2474–2481.
- [7] P. Rodríguez, A. Luna, R. Santiago Muñoz-Aguilar, I. Etxeberria-Otadui, R. Teodorescu, and F. Blaabjerg, “A Stationary Reference Frame Grid Synchronization System for Three-Phase Grid-Connected Power Converters Under Adverse Grid Conditions”, *IEEE Transactions on Power Electronics* 27(1), 99–112, January 2012.
- [8] P. Rodríguez, A. Luna, I. Candela, R. Mujal, R. Teodorescu, and F. Blaabjerg, “Multiresonant Frequency-Locked Loop for Grid Synchronization of Power Converters Under Distorted Grid Conditions”, *IEEE Transactions on Industrial Electronics* 58(1), January 2011.
- [9] P. Rodríguez, J. Pou, J. Bergas, I.I. Candela, R.P. Burgos, and D. Boroyevich, “Decoupled double synchronous reference frame PLL for power converters control”, *IEEE Transactions on Power Electronics* 22(2), 584–592, 2007.
- [10] M. Sędkak, S. Styński, M.P. Kazmierkowski, and M. Malinowski, “Operation of four-leg three-level flying capacitor grid-connected converter for RES”, *IECON 2013 – 39th Annual Conference of the IEEE Industrial Electronics Society*.
- [11] M. Bobrowska, R.K. Jasiński, and M.P. Kazmierkowski, “Grid synchronization and symmetrical components extraction with PLL algorithm for grid connected power electronic converters – a review”, *Bull. Pol. Ac.: Tech.* 59(4), Nov. 2011.
- [12] D. Dong, B. Wen, D. Boroyevich, P. Mattavelli, and Y.O. Xue, “Analysis of Phase-Locked Loop Low-Frequency Stability in Three-Phase Grid-Connected Power Converters Considering Impedance Interactions”, *IEEE Transactions on Industrial Electronics* 62(1), January 2015.
- [13] S. Vazquez, J.A. Sanchez, M.R. Reyes, J.I. Leon, and J.M. Carrasco, “Adaptive Vectorial Filter for Grid Synchronization of Power Converters under Unbalanced and/or Distorted Grid Conditions”, *IEEE Transactions on Industrial Electronics* 61(3), 1355–1367, March 2014.
- [14] K.-J. Lee, J.-P. Lee, D. Shin, Dong-Wook, and H.-J. Kim, “A Novel Grid Synchronization PLL Method Based on Adaptive Low-Pass Notch Filter for Grid-Connected PCS”, *IEEE Transactions on Industrial Electronics* 61(1), 292–301, 2014.
- [15] F. Gonzalez-Espin, E. Figueres, and G. Garcera, “An Adaptive Synchronous-Reference-Frame Phase-Locked Loop for Power Quality Improvement in a Polluted Utility Grid”, *IEEE Transactions on Industrial Electronics* 59(6), 2718–2731, 2012.
- [16] P. Lipnicki, “Comparison of performance of synchronization algorithms for grid connected power electronics converters according to proposed evaluation quality criteria”, *Informatyka, Automatyka, Pomiar w Gospodarce i Ochronie Środowiska* 1, 62–65, 2014, DOI: 10.5604/20830157.1093209, <https://e-iapgoss.pl/resources/html/article/details?id=36957>.
- [17] P. Lipnicki, “The impact of voltage disturbances on grid synchronization of power electronics converters working in distributed generation systems”, *PhD Doctoral Dissertation, Lublin University of Technology*, 2014.
- [18] D. Zieliński, “Power converter synchronization in presence of grid disturbances”, *PhD Doctoral Dissertation, Lublin University of Technology*, 2017 (in Polish).
- [19] D. Zieliński, “Dynamic Power Control of the Grid Converters”, *Informatyka, Automatyka, Pomiar w Gospodarce i Ochronie Środowiska IAPGOS* 1, 2016, www.e-IAPGOS.pl, DOI: 10.5604/20830157.1194283 (in Polish).
- [20] T. Chmielewski, “Influence of digital filters in Voltage Oriented Control on the operational quality of grid-tied converters”, *PhD Doctoral Dissertation, Lublin University of Technology*, 2018.
- [21] T. Chmielewski, “Comb filters for harmonics control in grid connected power electronic converters applications”, *19th European Conference on Power Electronics and Applications, EPE 2017 ECCE Europe*, 2017 IEEE Xplore, DOI: 10.23919/EPE17ECCEEurope.2017.8099163.
- [22] W. Jarzyna, D. Zieliński, K. Zielińska, and K. Fatyga, “Reduction of voltage and power oscillation in the two-phase shorting of a grid inverter”, *19th European Conference on Power Electronics and Applications, EPE 2017 ECCE Europe, Warsaw, Poland, 11–14 September 2017*, DOI: 10.23919/EPE17ECCEEurope.2017.8099384.
- [23] M. Depenbrock, “Direct self-control (DSC) of inverter-fed induction machine”, *IEEE Transactions on Power Electronics* 3(4), 420–429, 1988.
- [24] K.P. Kovács and I. Rácz, “Transient Vorgänge in Wechselstrommaschinen”, Budapest, 1959.
- [25] F. Blaschke, “Das verfahren der feldorientierung zur regelung der asynchronmaschine”, *Siemens Forschungs- und Entwicklungsberichte* 1, 1972.
- [26] W.C. Duesterhoeft, M.W. Schulz, and E. Clarke, “Determination of Instantaneous Currents and Voltages by Means of Alpha, Beta, and Zero Components”, *Transactions of the American Institute of Electrical Engineers* 70(2), 1248–1255, July 1951, DOI: 10.1109/T-AIEE.1951.5060554.

- [27] F. Baradarani, M.R. Dadash Zadeh, and M. Amin Zamani, "A Phase-Angle Estimation Method for Synchronization of Grid-Connected Power-Electronic Converters", *IEEE Transactions on Industrial Power Delivery* 30(2), 827–835, April 2015.
- [28] M.P. Kaźmierkowski, R. Krishnan, and F. Blaabjerg, "Control in Power Electronics: Selected Problems", *Academic Press*, 2002.
- [29] W. Jarzyna, D. Zieliński, "The impact of converter's synchronization during FRT voltage recovery in two-phase short circuits", *Conference 2015: Selected Problems of Electrical Engineering and Electronics*, WZEE 2015; Kielce; Poland; 17–19 September 2015.
- [30] G. Fedele, C. Picardi, and D. Sgrò, "A Power Electrical Signal Tracking Strategy Based on the Modulating Functions Method", *IEEE Transactions on Industrial Electronics* 56(10), 4079–4089, October 2009.
- [31] J.A. Suul, A. Luna, P. Rodríguez, and T. Undeland, "Voltage-Sensor-Less Synchronization to Unbalanced Grids by Frequency-Adaptive Virtual Flux Estimation", *IEEE Transactions on Industrial Electronics* 59(7), July 2012.
- [32] Y. Han, M. Luo, X. Zhao, J.M. Guerrero, and L. Xu, "Comparative Performance Evaluation of Orthogonal-Signal-Generators-Based Single-Phase PLL Algorithms – a Survey", *IEEE Transactions on Power Electronics* 31(5), 3932–3944, 2016.
- [33] L. Hadjidemetriou, E. Kyriakides, and F. Blaabjerg, "A Robust Synchronization to Enhance the Power Quality of Renewable Energy Systems", *IEEE Transactions on Industrial Electronics* 62(8), 4858–4868, 2015.
- [34] K.-J. Lee, J.-P. Lee, D. Shin, D.-W. Yoo, and H.-J. Kim, "A Novel Grid Synchronization PLL Method Based on Adaptive Low-Pass Notch Filter for Grid-Connected PCS", *IEEE Transactions on Industrial Electronics* 61(1), January 2014.
- [35] W. Jarzyna, P. Lipnicki, and D. Zieliński, "Synchronization of voltage frequency converters with the grid in the presence of notching", *COMPEL – The International Journal for Computation and Mathematics in Electrical and Electronic Engineering* 3(34), 657–673, 2015, DOI: 10.1108/COMPEL-10-2014-0266.
- [36] J. Ma, Y. Qiu, Y. Li, W. Zhang, Z. Song, and J.S. Thorp, "Research on the Impact of DFIG Virtual Inertia Control on Power System Small-Signal Stability Considering the Phase-Locked Loop", *IEEE Transactions on Power Systems* 32(3), 2094–2105, 2017.
- [37] K. Sakimoto, Y. Miura, and T. Ise, "Stabilization of a power system with a distributed generator by a Virtual Synchronous Generator function", *8th International Conference on Power Electronics – ECCE Asia*, 1498–1505, 2011, DOI: 10.1109/ICPE.2011.5944492.
- [38] R.K. Panda, A. Mohapatra, and S.C. Srivastava, "An Effective Inertia Control Scheme for Solar PV Systems with Conventional dq Controller", *2018 IEEE Power & Energy Society General Meeting (PESGM)*, DOI: 10.1109/PESGM.2018.8585529.
- [39] M. Malaczek and I. Wasiak, "Forming a microgrid to islanded operation as a mean to improve quality of supply in low voltage networks with distributed generation", *2018 18th International Conference on Harmonics and Quality of Power (ICHQP)*, 1–6, 2018.
- [40] P. Zielonka, M. Jasiński, M. Bobrowska-Rafał, and A. Sikorski, "Sterowanie przekształtnika sieciowego AC-DC podczas zapadów napięcia w sieci elektroenergetycznej, [Control fo AC-DC converter when voltage dips in supply line occurs]", *Przegląd Elektrotechniczny* 87(6), 79–84, 2011.
- [41] G. Wrona, M. Jasiński, M.P. Kaźmierkowski, M. Bobrowska-Rafał, and M. Korzeniewski, "Procesory zmiennoprzecinkowe serii TMS320F28xx w systemach sterowania przekształtników dla energetyki odnawialnej, (Floating Point DSP TMS320F28xx in control systems for Renewable Energy Sources RES)", *Przegląd Elektrotechniczny* 6, 2011.
- [42] P. Młodzikowski, A. Milczarek, S. Styński, M. Malinowski, and S. Kouro, "Control of simplified multilevel AC-DC-AC converter for small power generation systems", *2013 IECON Proceedings Industrial Electronics Conference*, 6700111, pp. 5951–5956.
- [43] M. Chen, L. Peng, B. Wang, and J. Kan, "PLL based on extended trigonometric function delayed signal cancellation under various adverse grid conditions", *IET Power Electronics* 11(10), 1689–1697, 2018.
- [44] A. Sikorski and M. Korzeniewski, "AC/DC/AC converter in a small hydroelectric power plant", *Bull. Pol. Ac.: Tech.* 59(4), 2011, DOI: 10.2478/v10175-011-0062-6.
- [45] G.A. Leonov, N.V. Kuznetsov, and E.P. Solovyeva, "A simple dynamical model of hydropower plant: stability and oscillations", *ScienceDirect IFAC-PapersOnLine* 48–11 (2015) 656–661, Available online at www.sciencedirect.com.
- [46] Synchronization systems commercial offer, KARED Sp.z o.o., <http://www.kared.com.pl/en/contact.html>, 2019.
- [47] M. Szypulski and G. Iwański, "Synchronization of state-feedback-controlled doubly fed induction generator with the grid", *Bull. Pol. Ac.: Tech.* 66(5), 2018, DOI: 10.24425/125334.
- [48] A. Assenkamp, C. Kreischer, and S. Kulig, "Capability of synchronous machines to ride through events with high ROCOF", *Archives of Electrical Engineering* 68(2), 325–339 (2019), DOI 10.24425/ae.2019.128271.